

Research Paper

Simulating urban land growth by incorporating historical information into a cellular automata model

Haijun Wang^{a,b}, Jiaqi Guo^{a,*}, Bin Zhang^a, Haoran Zeng^a^a School of Resource and Environmental Sciences, Wuhan University, Wuhan, China^b Key Laboratory of Geographic Information System of MOE, Wuhan University, Wuhan, China

HIGHLIGHTS

- The temporal complexity of urban growth is considered in this paper.
- A CA model integrating smoothed transition rules (SM-Logistic-CA) is proposed.
- The SM-Logistic-CA model is shown to be superior to the standard Logistic-CA model.
- The expansion process and time of the historical period affect the simulation.
- The performance of the smoothed transition rules varies with the neighborhood size.

ARTICLE INFO

Keywords:

Urban growth
Temporal complexity
Historical information
Cellular automata
Expansion similarity index

ABSTRACT

The first and second laws of geography have been applied to the simulation of urban growth in many studies. However, by focusing on the spatial complexity of urban growth, these studies have the shared problem of ignoring the temporal complexity of urban growth, which can be solved by incorporating historical information into the simulation of urban growth. In this paper, we describe how we constructed a Logistic-CA model using smoothed transition rules (the SM-Logistic-CA model). Specifically, in this paper, we: 1) propose an expansion similarity index to measure the similarity of the urban expansion processes in two periods; 2) use linear smoothing and exponential smoothing to integrate the historical transition rules; 3) assign smoothing weights to each period based on the expansion similarity index; and 4) compare the SM-Logistic-CA model with the standard Logistic-CA model. The results show that the SM-Logistic-CA model can exhibit good control of urban growth, and can avoid the problem of new urban land expanding blindly along the original urban land when smoothing is performed using the transition rules of appropriate historical periods. The similarity of the expansion processes between the historical period and the target period and the temporal distance of the historical period from the target period affect the simulation accuracy of the SM-Logistic-CA model, and the neighborhood size changes the relative importance of these two factors on the simulation results.

1. Introduction

In the past few decades, rapid urbanization has swept many countries around the world, and has led to an upsurge of research on urban growth among scholars (Agyemang and Silva, 2019; Liu et al., 2014; Zhou et al., 2020). The cellular automata (CA) model is commonly used to simulate urban land expansion as it has the advantages of an open structure, flexible application, and ease of coupling with geographic information system (GIS) environments (Al-sharif and Pradhan, 2013; Ku, 2016;

Santé et al., 2010). The transition rules and the neighborhood configuration are the two key components that determine the simulation results of a CA model (Li and Liu, 2006; White and Engelen, 2000; Wu et al., 2012), where these two components respectively calculate the probability of a cell being converted into an urban land patch by mapping the urban land expansion drivers, and the interaction between the land-use types. Many methods have been proposed to extract transition rules, such as logistic regression (Wu and Yeh, 1997), Markov chain based methods (Palmate et al., 2017), the tree-based approach (Shafizadeh-

* Corresponding author at: School of Resource and Environmental Sciences, Wuhan University, Wuhan, Hubei, China.

E-mail addresses: landgiswhj@163.com (H. Wang), gjq1412@163.com, gjq1412@whu.edu.cn (J. Guo), landgiszb@whu.edu.cn (B. Zhang), zenghaoran@whu.edu.cn (H. Zeng).

Moghadam et al., 2017b), neural networks (Li and Yeh, 2001), heuristic algorithms (Feng et al., 2011; Liu et al., 2008), and their combination (Ma et al., 2020; Sun et al., 2018). Among these methods, logistic regression is one of the most popular methods among researchers because it is easy to implement and explain (Cao et al., 2020; Mustafa et al., 2018). The neighborhood configuration, which is made up of the neighborhood structure, neighborhood size, and neighborhood weight, has been studied extensively and in depth. The Moore type is one of the most frequently used neighborhood structures in the related research, and many studies have shown that the neighborhood size can have a significant influence on the simulation accuracy (Kocabas and Dragicevic, 2006a; Shafizadeh-Moghadam et al., 2017a; Wu et al., 2012). In addition, in some studies, the functions of the neighborhood have been enriched by using an enrichment factor or a dual-scale neighborhood in the simulation (Liao et al., 2016; Verburg et al., 2004; Zhang and Wang, 2021).

Urban growth is a complex process (He et al., 2006), which is affected by many factors, such as social and economic factors, physical geography factors, and policy preferences. As a geographical phenomenon, the process of urban expansion and evolution should conform to the universal laws, i.e., the first and second laws of geography. The first law of geography can be summed up as “spatial correlation”, i.e., “everything is related to everything else, but near things are more related to each other” (Tobler, 1970). The second law of geography can be summarized as “spatial heterogeneity”, i.e., “geographic variables exhibit uncontrolled variance” (Goodchild, 2004). These two laws have been taken into account in constructing simulation models of urban growth, and many practical studies have been conducted on this basis. For example, by considering the distance decay effect of a cellular neighborhood (Liao et al., 2014; Ziaeef Vafaeyan et al., 2018), researchers have assigned the neighborhood cells closer to the center cell a greater weight in the application of the CA model. This initiative has incorporated spatial correlation into the simulation. Other studies have used local models, such as geographically weighted regression (GWR) (Feng and Tong, 2018; Mirbagheri and Alimohammadi, 2017), to extract the transition rules of an urban growth CA model. There have also been some studies that have constructed different transition rules for different regions by “partitioning” (Qian et al., 2020; Xia and Zhang, 2021). The use of these methods introduces spatial heterogeneity into the urban growth simulation. However, by focusing on the spatial complexity of urban growth, these studies have the shared problem of ignoring the temporal complexity of urban growth, which can be solved by incorporating historical information into the simulation of urban growth. A recently published paper took the influence of time into account in the simulation of urban growth by constructing a trend-adjusted neighborhood CA model (Li et al., 2020), which is an approach that takes into account the differences in the impact of time when urban land is developed. However, the performance of the model is affected by the urban expansion pattern, and continuous annual land-use data are not easily available.

In addition to the above-mentioned laws that are already well known to scholars, Zhu et al. (2018) proposed the law of “geographical similarity”, which can be described as: the more similar the geographic configurations of two points (areas), the more similar the values (processes) of the target variable at these two points (areas) will be. It has been proved that this law can be regarded as the third law of geography, in terms of its universality, independence, and application (Zhu et al., 2020). However, two questions remain with regard to geographical similarity. Can we find any phenomena related to geographical similarity in the process of urban growth? How do we characterize geographical similarity in the simulation? The similarity law proposed by Zhu et al. describes the possible association between two regions from a spatial perspective. If this could be depicted in temporal terms, i.e., the more similar the geographic configuration (such as the urban growth driving mechanisms) in two time periods of the same region, the more similar the geographical processes (e.g., urban growth) in the two

periods will be. Furthermore, some scholars have proposed that a wide range of historical information should be considered in the simulation of urban growth (Aburas et al., 2016). For example, Fu et al. (2018) used logistic regression models fitted by a single driving factor and the land-use changes between two time points to select effective driving factors in land-use simulation, and used the logistic regression results as the input for multi-criteria evaluation (MCE), to solve the problem of the lack of connection with local historical data when using MCE for simulation. Integrating multiphase historical transition rules is an idea which considers the temporal complexity of urban growth in the simulation, based on the similarity law from the temporal perspective. Although the driving mechanisms of urban growth may change over time, the transition rules extracted from multiple historical periods that have a similar expansion process to the target research period may help to achieve a better simulation. This is because, in the same region, if the driving mechanisms of urban growth in the two time periods are similar, the urban expansion processes in the two periods are more likely to be similar. The historical transition rules may contain some hidden information that will affect the future urban land-use change. Unfortunately, this information is difficult to express in mathematical formulas or natural language.

This study was aimed at exploring the effect of incorporating historical information into the CA simulation of urban expansion, and the following two questions were considered in depth: 1. What influence will the integration of historical transition rules have on the simulation results? 2. What factors can make a CA model using smoothed transition rules achieve a more realistic simulation? These questions have rarely been considered in previous studies. Clarifying the answers will provide a new perspective for the study of urban landscape change, and may have great implications for a better understanding of the influencing factors in the urban expansion process.

2. Methods

In this study, logistic regression was used to extract the transition rules, and random sampling was conducted for the developed cells and undeveloped cells. The ratio of developed sample points to undeveloped ones was 1:1. After the transition rules of each period were obtained, weights were assigned to them to obtain the smoothed transition rules, in accordance with the expansion similarity index. The iteration number for the CA simulation was set to 20, and the simulation process was implemented in MATLAB. The analytical framework of this study is shown in Fig. 1, and the main methods are as follows.

2.1. The expansion similarity index

The problem of “similarity” has been widely studied in economics (Juszczuk et al., 2020), biology (Zheng et al., 2020), and computer science (Lastra-Díaz et al., 2019), but the measurement methods for “similarity” in these fields have mostly been aimed at static data without spatial attributes. Measures for landscape similarity do exist (Niesterowicz and Stepinski, 2016), but they cannot indicate the similarity of the urban expansion, which is a dynamic process. In order to measure the similarity of the urban expansion process, the characteristics of urban expansion need to be quantified.

The landscape expansion index (LEI) proposed by Liu et al. (2010) is considered to be a landscape index that can measure the dynamic process of urban growth, and has been applied in many cases. To be specific, the LEI is obtained by constructing buffer zones for each newly grown urban patch, and then calculating the proportion of the existing urban land in the buffer zones (Eq. (1)). The LEI can be used to determine which of the three expansion patterns (i.e., “infilling”, “edge-expansion”, and “outlying”) each new urban patch belongs to, and to identify the differences of the expansion characteristics among patches at the micro scale. In addition, the area-weighted mean expansion index (AWMEI, Eq. (2)), which was extended from the LEI by Liu et al. (2010),

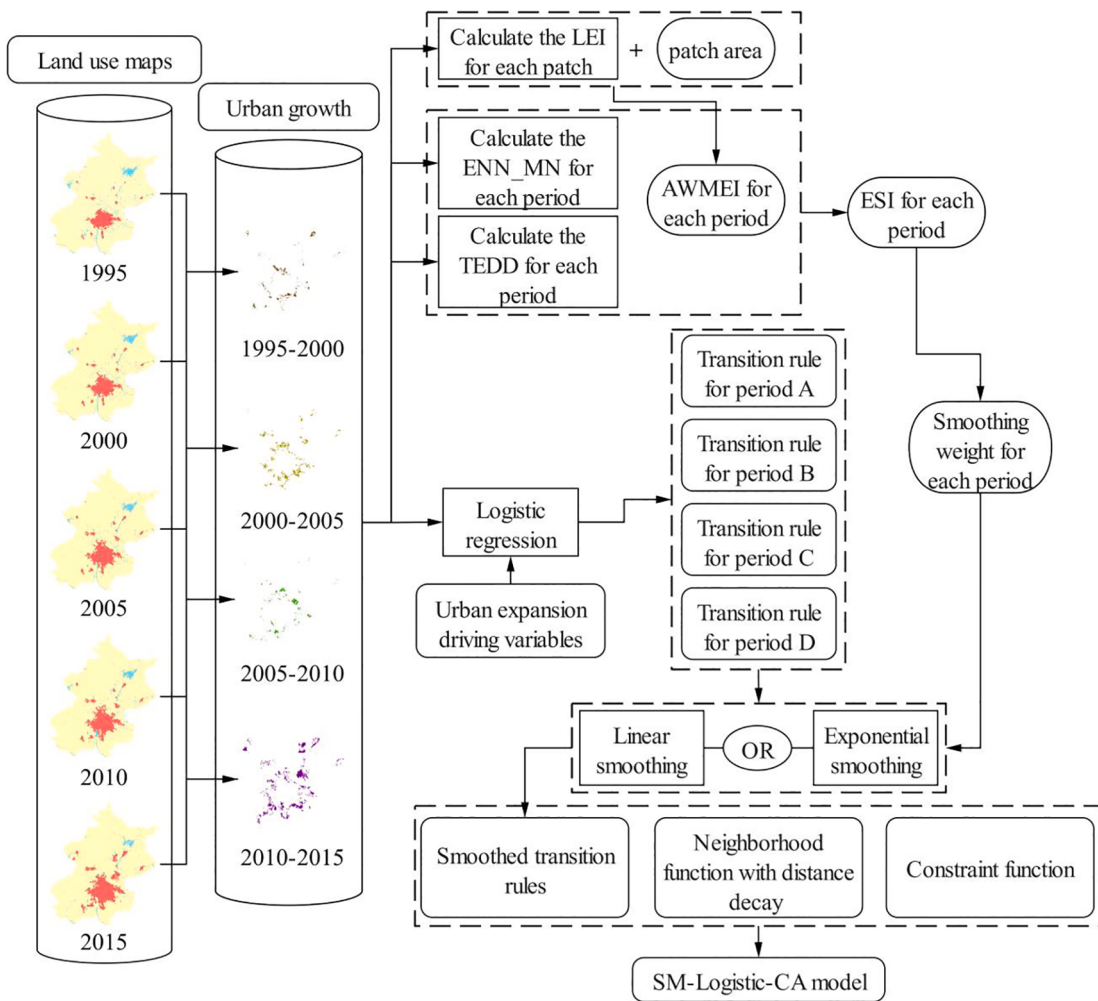


Fig. 1. The analytical framework.

can be used to analyze whether urban growth is in the diffusion stage or the fusion stage, at the global scale.

$$LEI = 100 \times \frac{A_u}{A_u + A_n} \quad (1)$$

where A_u is the area of urban land in the buffer zone, and A_n is the area of non-urban land in the buffer zone.

$$AWMEI = \sum_{i=1}^N LEI_i \times \left(\frac{a_i}{A} \right) \quad (2)$$

where N is the total number of new patches, LEI_i is the LEI of the i th new patch, a_i is the area of the i th new patch, and A is the total area of the new patches.

Although the AWMEI can denote the expansion pattern characteristics of newly grown urban land, in order to fully quantify the characteristics of urban expansion, we used FRAGSTATS to calculate the mean Euclidean nearest-neighbor distance (ENN_MN) of the newly grown urban patches in each period, to quantify the spatial distribution of new urban patches (McGarigal and Marks, 1995). The ENN_MN is usually used as an index to measure the fragmentation of the landscape, and it has the advantage that it is not sensitive to the patch size and can obtain more reliable results (Hargis et al., 1998; Zhao et al., 2014). Eq. (3) expresses the calculation of the ENN_MN, which is the indicator used for measuring the expansion distribution characteristics:

$$ENN_MN = \frac{\sum_i^N h_i}{N} \quad (3)$$

where h_i is the distance (m) from patch i to the nearest-neighbor patch of the same type, and N is the total number of new patches.

In addition, equal-fan analysis (Sun et al., 2020) was used to calculate the total expansion direction difference (TEDD) between the newly grown urban patches in the historical period and in the target period, to identify the expansion direction characteristics. Specifically, a suitable point was treated as the center (the municipal administrative center was used in this study), and a circular buffer area that can cover all the newly grown urban patches was made. We then divided the buffer area into 16 equal parts (as shown in Appendix A). The percentage of the newly added urban land area in each direction was calculated with regard to the total newly grown urban area, and we then calculated the difference with the corresponding value of the target period, and calculated the sum of the absolute values of the difference to obtain the TEDD, as shown in Eq. (4):

$$TEDD = \sum_{j=1}^{16} \left| \left(\frac{a_P^j}{A_P} \right) - \left(\frac{a_Q^j}{A_Q} \right) \right| \quad (4)$$

where a_P^j and a_Q^j are the area of new urban patches in a certain direction j of period P and period Q, respectively; and A_P and A_Q are the total area of new urban land in period P and period Q, respectively.

Eq. (5) was used to combine the AWMEI, ENN_MN, and TEDD

metrics to form the relative expansion feature index (REFI). In Eq. (5), “[]_P” represents the indicators of a certain period, and “[]_Q” represents the indicators of the target period.

$$\text{REFI}_P = \frac{[\text{AWMEI} \cdot \text{ENN_MN} \cdot (1 + \text{TEDD})]_P}{[\text{AWMEI} \cdot \text{ENN_MN} \cdot (1 + \text{TEDD})]_Q} \quad (5)$$

As mentioned earlier, the three indicators measure the characteristics of urban expansion from the three aspects of the expansion pattern, the expansion distribution, and the expansion direction, and the AWMEI also considers the influence of the patch area, so that the REFI can fully capture the characteristics of urban expansion. The similarity between the expansion process of the historical period and that of the target period can be measured by the difference between the two REFIs. The greater the difference, the lower the similarity. Based on this, the expansion similarity index (ESI) was proposed, as shown in Eq. (6), where the larger the value of the ESI, the more similar the urban expansion of the historical period is to that of the target period.

$$\text{ESI}_{(PQ)} = 10 - (|\text{REFI}_P - \text{REFI}_Q|) \quad (6)$$

2.2. Linear smoothing and exponential smoothing

To consider the influence of historical transition rules in the simulation of urban growth, we referred to the suggestions of Huang et al. (2009), i.e., the transition rules obtained from the logistic regression were smoothed by Eq. (7), and then logit transformation (Eq. (8)) was applied to the smoothed results to obtain the transition probability for the cells (P^L).

$$\text{Logit}(P) = w_1 \cdot \text{Logit}(P)_1 + w_2 \cdot \text{Logit}(P)_2 + \dots + w_n \cdot \text{Logit}(P)_n \quad (7)$$

In Eq. (7), w_n represents the weight in the corresponding period, and $\text{Logit}(P)_n$ represents the result of the logistic regression in the corresponding period.

$$P^L = \frac{1}{1 + e^{-\text{Logit}(P)}} \quad (8)$$

The key to smoothing multiple transition rules is to determine the weight of each period. The weight in linear smoothing is directly calculated from the value of the ESI. In other words, the weight of a period in linear smoothing is equal to the proportion of its ESI to the sum of all the periods, i.e.,

$$w_i = \frac{\text{ESI}_i}{\text{ESI}_1 + \dots + \text{ESI}_i + \dots + \text{ESI}_n} \quad (9)$$

Single exponential smoothing (Cadenas et al., 2010), double exponential smoothing (Wu et al., 2016), and triple exponential smoothing (Jiang et al., 2020) are common types of exponential smoothing. In this study, we adopted the relatively simple single exponential smoothing method. The formula for single exponential smoothing is:

$$S_t = \alpha \cdot y_{t-1} + (1 - \alpha) \cdot S_{t-1}, 0 < \alpha \leq 1, t \geq 3 \quad (10)$$

where S represents the exponential smoothed value, α is a constant parameter, y represents the original observation value, and t represents the smoothing period. S_2 is equal to y_1 , and there is no S_1 .

In this study, the purpose of using exponential smoothing was to obtain a set of weights, rather than making predictions about the data, which is the most common purpose when exponential smoothing is used (Sadeghi, 2015). Some adjustments were made to the single exponential smoothing method to make it suitable for smoothing the transition rules, i.e., every period was reordered in accordance with its ESI. Specifically, once we determined the value of α , a set of exponential smoothing weights could be obtained from Eq. (10). The transition rule extracted from the period with the largest ESI was then treated as the “y” with the largest weight, and the transition rule of the period with the smallest ESI was taken as the “y” with the smallest weight. The other transition rules were given the corresponding weights according to the ESI of their

periods. The ESI determines the smoothing order of the rules in Eq. (10), and the order determines the weight of each rule, so that the ESI indirectly determines the smoothing weight of each rule in exponential smoothing.

2.3. The smoothed logistic cellular automata (SM-Logistic-CA) model

The influence intensity of urban cells in the neighborhood on the central cell will decrease with increasing distance from the central cell, which has been recognized by many scholars. (Liao et al., 2014; Roodposhti et al., 2020). In this study, we selected a relatively simple inverse distance decay function (de Mesnard, 2013) to characterize the influence intensity of neighborhood cells at different distances from the central cell. The neighborhood function coupled with the inverse distance decay function is expressed as:

$$P^N = \frac{\sum_{n \times n} \omega_d \cdot CS(d)}{n \times n - 1} \quad (11)$$

where n represents the neighborhood size; d represents the distance between the neighborhood cell and the central cell, where $d = 1, 2, 3, \dots, \frac{n+1}{2}$; ω_d represents the inverse distance decay weight, where $\omega_d = \frac{d^{(-1)}}{\sum d^{(-1)}}$; and $CS(d)$ represents the neighborhood cell state function when the distance from the central cell is d . If the neighborhood cell is an urban cell, 1 is returned; otherwise, 0 is returned. The random perturbation term is not adopted in the calculation of the final transition probability of the cell as it can disrupt the simulation results. When the cell is a developed urban cell or a water cell, the constraint function $CON()$ returns 0; otherwise, it returns 1. The final transition probability of the SM-Logistic-CA model constructed in this study is then:

$$P = P^L \cdot P^N \cdot CON() \quad (12)$$

3. Experiments and results

3.1. Study area

As the political and cultural center of China, Beijing enjoys vast opportunities for investment, which has contributed to the acceleration of the urbanization process. By the end of 2019, the number of permanent residents was more than 20 million, of which more than 85% were urban residents. As of 2018, Beijing covered a total area of 16,410.54 km². In recent years, the urban land of Beijing has been rapidly expanding (Fig. 2 (b)), causing “big-city diseases” such as traffic congestion and air pollution. In order to curb the blind spread of urban land, the General Urban Plan of Beijing (2016–2035) sets the goal of reducing the scale of urban and rural construction land (http://www.beijing.gov.cn/gongkai/guihua/wngh/cqgh/201907/t20190701_100008.html). Understanding the influence of the historical transition rules can help us to fully grasp the expansion mechanism of urban land, which is essential information for government to rationally plan new urban land and to limit the blind growth of urban land.

3.2. Data sources and preparation

In this study, raster land-use data were used to analyze the urban land-use change, and 1995, 2000, 2005, 2010, and 2015 were selected as the time nodes. The spatial distribution of the urban land use was obtained from the raster land-use data (30 m × 30 m) in these five years. In addition, population and gross domestic product (GDP) (1 km × 1 km) spatial data, road vector data, digital elevation model (DEM) data (1 km × 1 km), and the locations of the administrative centers at the county level in Beijing were also used as the driving factors for urban land growth, which have all been proven effective in published studies (Aburas et al., 2016; Feng et al., 2019).

All the data mentioned above were obtained from the Resource and

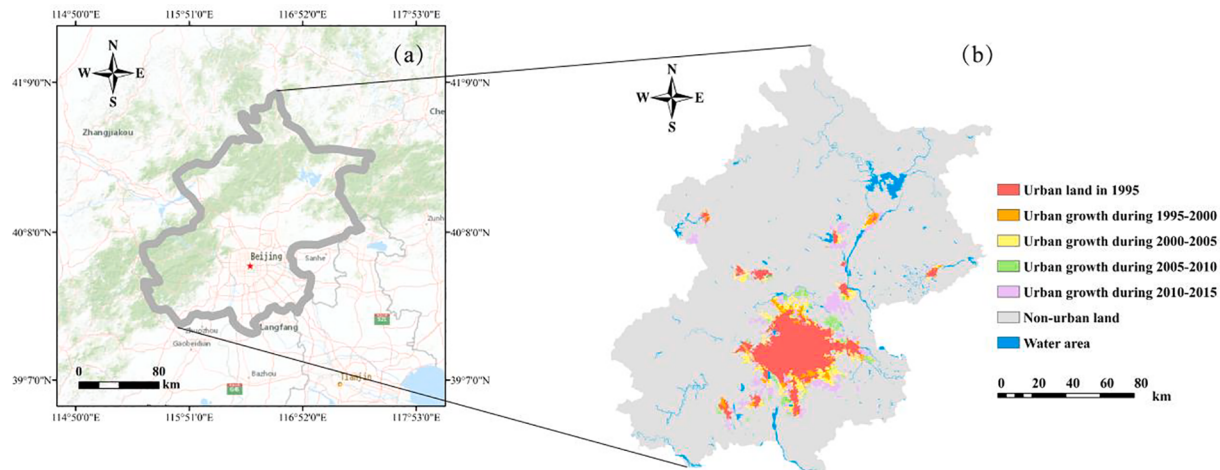


Fig. 2. The location of Beijing (a). The urban growth of Beijing during each five-year period from 1995 to 2015 (b).

Environment Science and Data Center of the Chinese Academy of Sciences (<http://www.resdc.cn/>). The original land-use data were reclassified into three categories—urban land, non-urban land, and water surface—in ArcGIS 10.5. Resampling was used to unify the resolution of all the raster data to 30 m × 30 m. The DEM data and the locations of the administration centers could be regarded as unchanged over the 20 years of this study. The road data were from 2015, as this was the only

available year. By using the “Euclidean Distance” tool of ArcGIS 10.5, we obtained the distance variables of railway, super highway, national highway, provincial highway, county highway, existing urban land, and county administrative centers. The urban growth driving variables are shown in Fig. 3, and the names and coefficients of the urban growth driving variables are listed in Table 1. The land-use data in vector format were generated using the ArcGIS “Raster to Polygon” tool for calculating

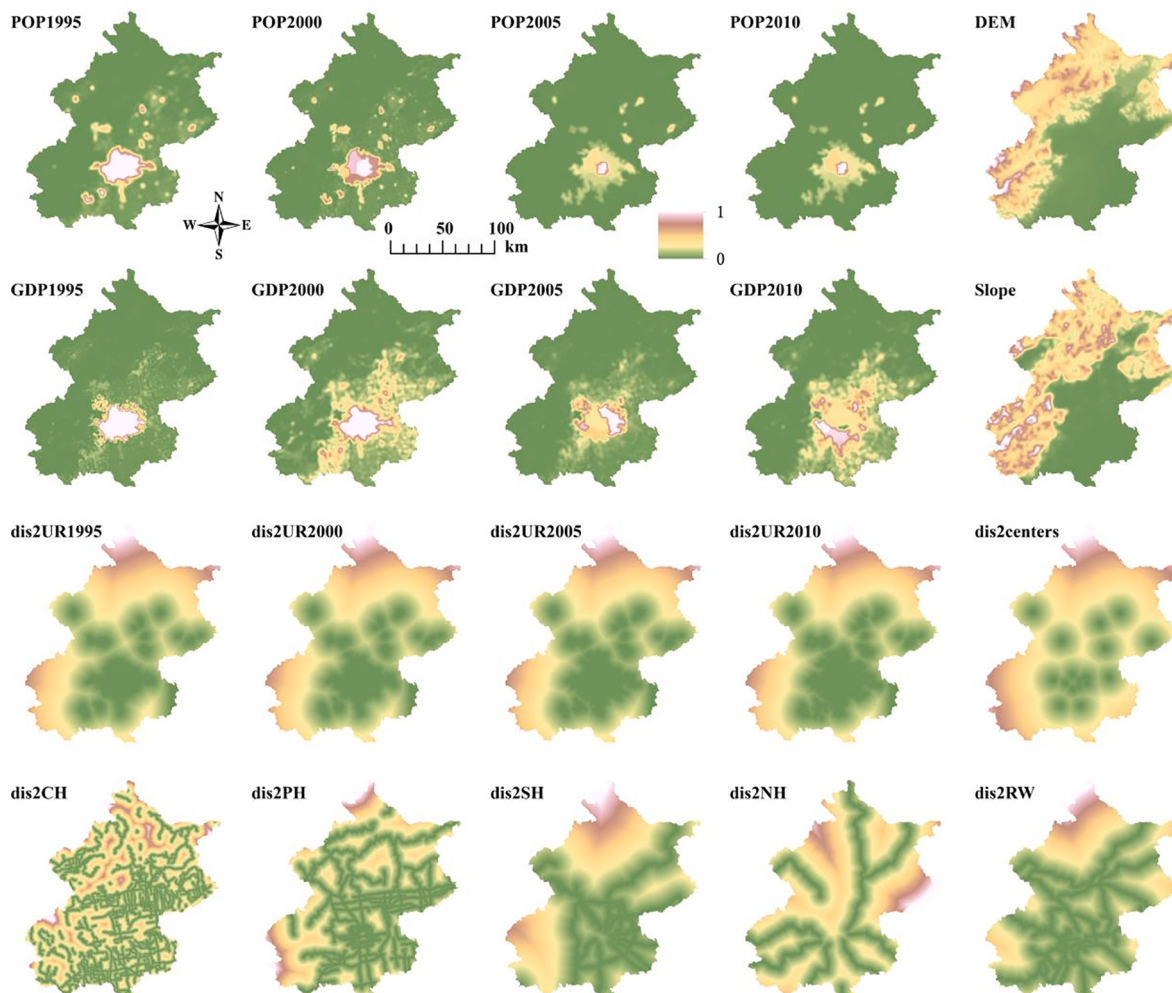


Fig. 3. Urban growth driving variables.

Table 1

Meanings of the urban growth driving variable names and the logistic regression coefficients for each period.

The variable name	Meaning	1995–2000	2000–2005	2005–2010	2010–2015
POP	Population	-1.266**	-3.248***	-10.048***	-4.689***
GDP	Gross domestic product	-3.355***	-1.675***	0.287	3.519***
DEM	Elevation	1.129	-15.930***	-12.151***	4.866***
Slope	Slope	-5.873***	-0.050	-3.019**	-3.889***
dis2centers	Distance from county administrative centers	8.726	2.085**	4.301***	-1.476***
dis2UR	Distance from existing urban land	-82.005***	-72.550***	-60.867***	-29.766***
dis2CH	Distance from county highway	2.797**	-3.279***	2.122*	-0.641
dis2PH	Distance from provincial highway	-2.337	2.761**	10.138***	-4.556***
dis2SH	Distance from super highway	-15.089***	-1.766	-2.602	-3.161***
dis2NH	Distance from national highway	3.859***	0.139	-0.988**	-0.287
dis2RW	Distance from railway	-26.575***	-4.503***	2.706	-3.361***
constant		4.016***	4.303***	2.066***	2.068***

Note: *** indicates that the variable is significant at $p < 0.01$; ** indicates that the variable is significant at $p < 0.05$; * indicates that the variable is significant at $p < 0.1$.

the LEI.

3.3. The expansion similarity index and smoothing weight

From 1995 to 2000 is denoted as urban growth period A, and from 2000 to 2005 is denoted as period B, and so on. In this way, four periods were obtained. According to the number of newly developed cells in each period, 2952, 5894, 2640, and 9980 points were sampled for periods A, B, C, and D, respectively (Zhang and Xia, 2021). The period from 2010 to 2015 (i.e., period D) was considered as the target research period, and the remaining three periods were considered as the historical periods. Liu et al. (2010) developed an ArcGIS plug-in (downloadable from <http://www.geosimulation.cn/LEI.html>) to calculate the LEI of each newly developed urban patch. We referred to the research results of Liu et al. (2010), and set the buffer distance as 1 m when the LEI was calculated. The ESI of each period (Table 2) was then calculated in accordance with Eq. (6). As mentioned previously, the weights of each period in the linear smoothing were directly determined by the ESI (Eq. (9)), as shown in Table 3.

On the one hand, exponential smoothing requires data of no less than three periods to make it different from linear smoothing. On the other hand, the purpose of using exponential smoothing is to provide an alternative method for the determination of the smoothing weights. Therefore, the exponential smoothing uses four transition rules, and serves as the control group for “linear-ABCD”. The key to exponential smoothing is to determine the value of parameter α (Su et al., 2018). We adopted an experimental method to determine the value of α , while setting the step size as 0.1. The simulation was conducted with all the combinations of α and neighborhood sizes, taking the figure of merit (FoM) as the evaluation index. The results are listed in Appendix B, where it can be seen that half of the neighborhood sizes have the highest accuracy when $\alpha = 0.4$, so we used $\alpha = 0.4$ to calculate the weights in the exponential smoothing.

3.4. Evaluation of the simulation results

The all transition rules were used to simulate the urban growth of Beijing from 2010 to 2015. Based on the transition rule extracted from period D (namely rule10_15), we verified how the smoothed transition rules, which contained the historical information, affected the simulation results for the target period. The five indicators of the overall accuracy, Kappa coefficient, FoM, producer's accuracy, and user's

Table 2

The expansion similarity index for the four periods.

Periods	1995–2000 (Period A)	2000–2005 (Period B)	2005–2010 (Period C)	2010–2015 (Period D)
ESI	9.4790	8.5709	6.5241	10

Table 3

Weights of each period in different transition rules.

Periods	Transition rules				
	rule10_15	linear-ABCD	linear-BCD	linear-CD	exp-ABCD
Period A	0	0.2742	—	—	0.24
Period B	0	0.2479	0.3415	—	0.216
Period C	0	0.1887	0.2600	0.3948	0.144
Period D	1	0.2892	0.3985	0.6052	0.4

Note: “rule10_15” is an unsmoothed transition rule. Names beginning with “linear” are smoothed linearly, names beginning with “exp” are smoothed exponentially, and the suffix letters indicate which periods were used for the smoothing. For example, “linear-BCD” refers to a transition rule that uses transition rules extracted from periods B, C, and D and undergoes linear smoothing.

accuracy are used in this paper to evaluate the simulation results. These indicators were found to be highly consistent in judging the pros and cons of the different results (see Table 4), and the same applied in the case of other neighborhood sizes. Therefore, the representative FoM was selected as the comparison indicator for the simulation accuracy. Early studies showed that the neighborhood size has an impact on the simulation accuracy (Kocabas and Dragicevic, 2006b). In this study, the classical extended Moore neighborhood (5×5) was used as the initial size. The neighborhood was then gradually expanded to explore whether the performance of the smoothed transition rules changed in the case of different neighborhood sizes. The FoM values of the simulation results, which were obtained through the parameter combinations of each transition rule and neighborhood size, are listed in Table 5.

It can be seen that when the neighborhood size is fixed, using the smoothed transition rule can increase the FoM by 0.71% (in the case of the 11×11 neighborhood, the FoM of “rule10_15” and “exp-ABCD” are compared) at most. However, when the neighborhood is expanded (from 5×5 to 35×35) and the smoothed transition rule (linear-BCD) is used at the same time, the FoM increases by up to 1.62%.

In order to more intuitively show the difference between the

Table 4

Accuracy evaluation of all the transition rules under a neighborhood size of 5×5 .

Transition rules	Evaluation indicators				
	Overall accuracy	Kappa	FoM	Producer accuracy	User accuracy
rule10_15	0.9803	0.8197	0.2032	0.2684	0.4554
linear-ABCD	0.9806	0.8218	0.2090	0.2747	0.4661
linear-BCD	0.9805	0.8215	0.2080	0.2737	0.4644
linear-CD	0.9802	0.8184	0.1997	0.2646	0.4490
exp-ABCD	0.9806	0.8218	0.2090	0.2747	0.4662

Table 5

FoM values of the simulation results under different combinations of transition rule and neighborhood size.

Transition rules	Neighborhood sizes							
	5 × 5	11 × 11	15 × 15	21 × 21	25 × 25	31 × 31	35 × 35	41 × 41
rule10_15	0.2032	0.2056	0.2084	0.2116	0.2133	0.2142	0.2141	0.2135
linear-ABCD	0.2090	0.2125	0.2148	0.2171	0.2177	0.2175	0.2170	0.2160
linear-BCD	0.2080	0.2115	0.2148	0.2174	0.2185	0.2193	0.2193	0.2186
linear-CD	0.1997	0.2022	0.2055	0.2082	0.2094	0.2110	0.2111	0.2103
exp-ABCD	0.2090	0.2127	0.2153	0.2177	0.2186	0.2186	0.2178	0.2165

simulation results of the smoothed and unsmoothed transition rules, we selected three local areas of different sizes in the study area and compared the simulation results of each transition rule with the reality (Fig. 4). Clearly, it can be seen that the smoothed transition rules “linear-ABCD” and “exp-ABCD” have more fine control over the urban land growth, and the edge of the simulation results is closer to the reality. For the simulation result of “rule10_15”, most of the new urban land expands along the edge of the original urban area, which is even more apparent in the simulation result of “linear-CD”. In the simulation results of these two cases, the boundary of the urban land is relatively rounded, which is far from the actual situation. The simulation result of “linear-BCD” is inferior to those of “linear-ABCD” and “exp-ABCD”, and is superior to those of “rule10_15” and “linear-CD”.

3.5. Sensitivity analysis for the SM-Logistic-CA model

It can be seen from Table 5 that the mutable components of the CA model, i.e., the transition rules and the neighborhood sizes, affect the simulation accuracy. It is therefore necessary to understand the sensitivity of the CA model to these two components.

3.5.1. Sensitivity to the transition rules

Generating different smoothed transition rules is a process of differentiating the influence intensity of the historical transition rules on the future urban growth simulation, which inevitably leads to different results. To explore the effectiveness of the different smoothed transition rules applied to the urban growth simulation in the target research period, we compared the FoM values of the smoothed transition rules

with the FoM value of the unsmoothed transition rule (rule10_15) when the neighborhood size was fixed, as shown in Fig. 5.

First of all, it is clear that the simulation effect of “linear-CD” is not good. No matter how large the neighborhood is, the simulation accuracy of “linear-CD” is worse than that of “rule10_15”. This is due to the fact that period C (2005–2010) has a low ESI, i.e., the expansion process of period C is quite different from that of target period D. Therefore, the transition rule of period C may have a negative impact on period D. Except for “linear-CD”, the accuracies of the other smoothed transition rules are better than that of “rule10_15”, which shows that considering the historical rules of urban growth can help us to achieve a more accurate simulation. In addition, if we compare “linear-ABCD” and “exp-ABCD”, it can be found that, no matter how large the neighborhood is, the simulation effect of “exp-ABCD” is better than that of “linear-ABCD”. This indicates that the relationship between the optimal weight of each period and its ESI is not linear. The essential difference between exponential smoothing and linear smoothing lies in the way that the smoothing weights are calculated. Therefore, when the historical periods are selected, determining the appropriate weight combination is vital to achieving a more accurate simulation.

3.5.2. Sensitivity to the neighborhood size

In order to intuitively understand the variation of the simulation accuracy as the neighborhood size changes, we calculated the improvement in the FoM for each neighborhood size by comparing it with the 5 × 5 size, the results of which are plotted in Fig. 6. It can be seen that, no matter which transition rule is used, with the increase of the neighborhood size, the improvement in FoM first increases and then decreases.

The influence of changing the neighborhood size was further explored, and the difference values of the FoM of two adjacent neighborhood sizes are plotted in Fig. 7. It can be found that, regardless of the transition rule used, the improvement in accuracy when expanding the neighborhood size is limited, and the improvement in FoM tends to

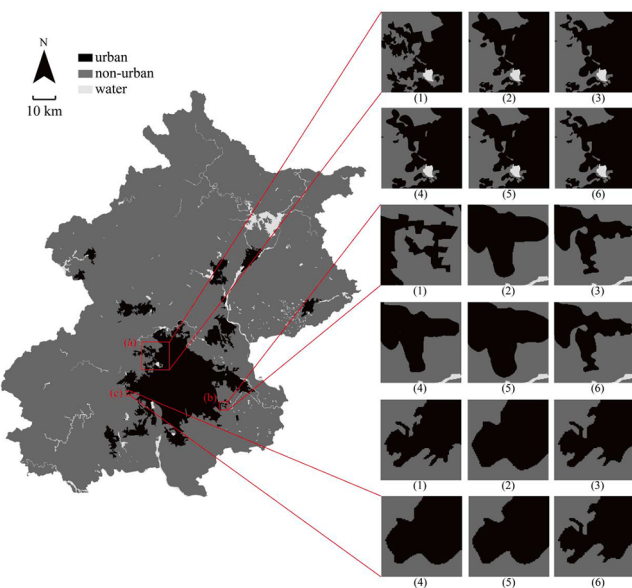


Fig. 4. Local comparison between the simulation results and reality. (All cases are under the 5 × 5 neighborhood size. Case (1) is the reality, and Cases (2)–(6) are the simulation results obtained using “rule10_15”, “linear-ABCD”, “linear-BCD”, “linear-CD”, and “exp-ABCD” as the transition rules, respectively.)

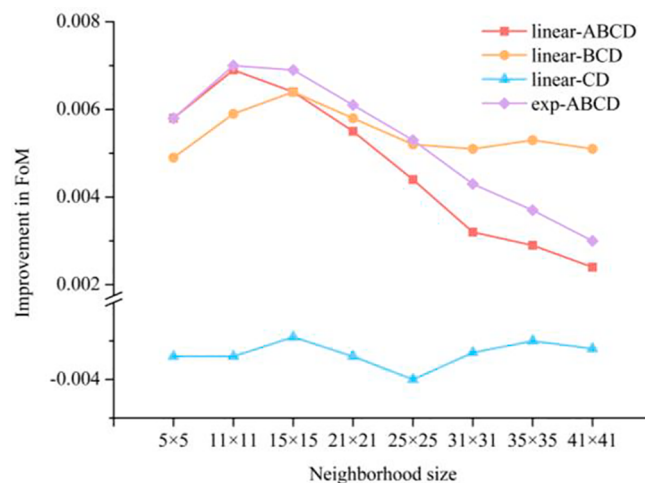


Fig. 5. Improvement in FoM compared to the unsmoothed transition rule (“rule10_15”).

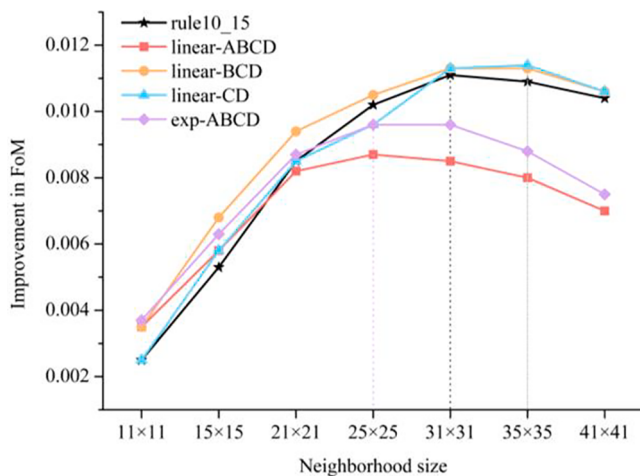


Fig. 6. Improvement in FoM compared to the extended Moore type neighborhood.

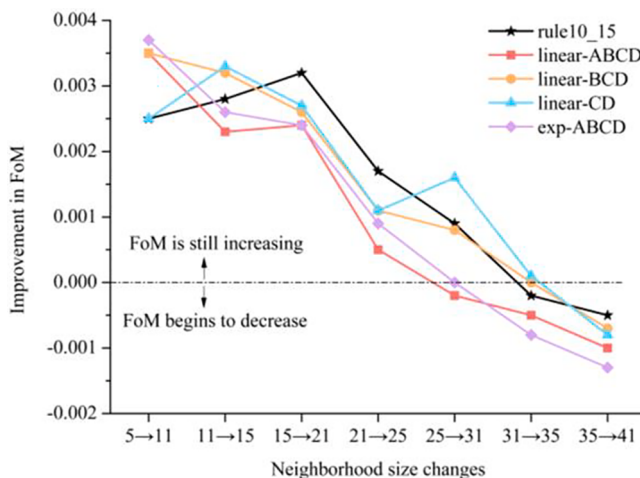


Fig. 7. Improvement in FoM when the neighborhood size changes.

decrease from an overall perspective.

4. Discussion

4.1. The impact of the attributes of the historical period on the simulation

According to the above analysis, the historical transition rules do affect the simulation result of urban expansion in the target period, and the simulation effect is significantly influenced by the selected historical periods. The influence mechanism of the historical periods is discussed below. Firstly, as described in Section 3.5.1, the similarity between the urban expansion process in the historical period and that in the target period will affect the simulation accuracy of the target period. Secondly, compared with "linear-ABCD", "linear-BCD" excludes historical period A, which has the highest ESI but is the oldest when compared with the other historical periods. By comparing the simulation results for these two rules, we find that the simulation accuracy of "linear-BCD" exceeds that of "linear-ABCD" as the size of the neighborhood increases. That is say, the influence of the temporal distance from the historical period to the target period can exceed the influence of the expansion similarity as the neighborhood size increases. Based on the two above-mentioned points, we can make the following reasonable conjecture: Two attributes of the historical period affect the simulation of the target period: 1) the similarity of the expansion processes of the two periods; and 2) the

temporal distance from the historical period to the target period. In order to verify the conjecture, we excluded period C, which had the lowest ESI value, and the transition rules of periods A, B, and D were used for the linear smoothing, with the smoothed transition rule named "linear-ABD". The smoothing weights for each period in "linear-ABD" and the simulation accuracies are listed in Table 6.

By comparing the FoM of "linear-ABCD" and "linear-ABD" in the case of the same neighborhood size (Fig. 8), we find that the simulation accuracy of "linear-ABD" is higher than that of "linear-ABCD" after excluding period C with a low ESI. This indicates that the similarity between the urban expansion process in the historical period and that in the target period does indeed influence the simulation effect for the target period. When the size of the neighborhood is less than 25×25 , "linear-ABD", which focuses on the similarity of the expansion process, obtains a higher simulation accuracy; when the size of the neighborhood is greater than or equal to 25×25 , "linear-BCD", which focuses on the temporal distance of the historical period, obtains a better simulation effect. This is consistent with the results of the earlier analysis in this section, so the conjecture in this section can be considered as scientific. In addition, the experimental results for "linear-ABD" in turn confirm that the ESI proposed in Section 2.1 can be used to correctly measure the similarity of urban growth processes in different periods.

4.2. The selection of indicators for measuring expansion similarity

Urban expansion is a continuous process, and historical land-use conditions may have potential effects on future urban land-use change, which has rarely been considered in previous studies. In this paper, we describe how a smoothing method was used to incorporate historical information into urban land expansion simulation. The smoothing weight was determined according to the degree of similarity between the expansion process of a certain historical period and that of the target period. We also proposed the ESI to measure urban expansion similarity. Referring to existing studies on urban expansion (Divigalpitiya & Handayani, 2015; Huang et al., 2020; Liu et al., 2016), the ESI can be quantified from three aspects, i.e., the expansion pattern characteristics, the expansion distribution characteristics, and the expansion direction characteristics. When selecting the sub-indicators of the ESI, two principles can be followed: 1) The value of the indicator should be affected by the number and the total area of newly grown urban patches as little as possible, which is due to the fact that urban land expands at different speeds in different development stages. In a rapid expansion stage, the number and the total area of new patches are much more than in a steady development stage. However, the urban expansion in the two periods may be similar due to the similar driving mechanisms. Therefore, the interference of the number and the total area of new patches on measuring the expansion similarity should be minimized as far as possible. 2) Each of the three kinds of ESI characteristics should be measured by an appropriate indicator to improve the performance of the ESI and avoid redundancy. For example, in this study, the expansion distribution characteristics were represented by the ENN_MN, which we found to be the most suitable indicator among the tested indicators, and is independent of the other selected indicators.

Based on the above two principles and many tests, the AWMEI, ENN_MN, and TEDD were selected as the sub-indicators of the ESI. The reasons for this choice are explained as follows. As a derivative of the LEI, the AWMEI can consider the effects of the patch area in the measurement of the expansion pattern, and is widely used to characterize the overall coalescence of patches (Tu et al., 2021). The patch density (PD) is commonly used to measure the spatial distribution of urban patches, and is defined as $PD = N/A$, where N is the number of patches, and A is the total landscape area (McGarigal and Marks, 1995). However, the total landscape area of each period was explicit in this study, which means that the PD actually indicates the number of new urban patches. Furthermore, there is no necessary connection between the number of new urban patches and the expansion similarity. Therefore,

Table 6

The weight of each period and the FoM of the simulation results for “linear-ABD”.

Weight	Period A	Period B	Period D			
FoM	0.3379	0.3056				
	Neighborhood sizes					
	5 × 5	11 × 11	15 × 15	21 × 21	25 × 25	31 × 31
	0.2097	0.2132	0.2157	0.2176	0.2182	0.2183
						35 × 35
						0.2178
						41 × 41
						0.2173

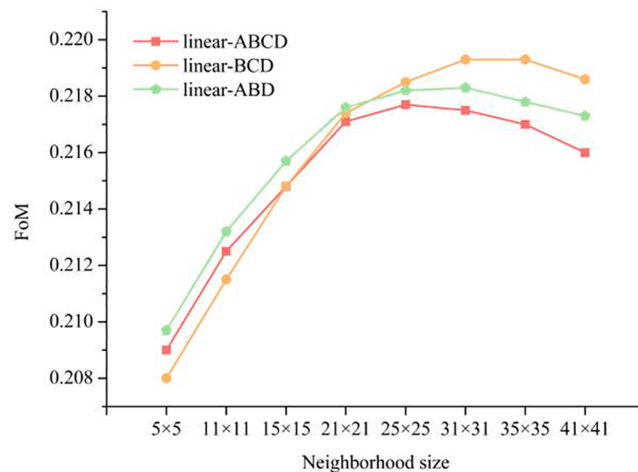


Fig. 8. The FoM of the simulation results for “linear-ABCD”, “linear-BCD”, and “linear-ABD”.

the ENN_MN is more suitable than the PD for the construction of the ESI. The equal-fan analysis can analyze the characteristics of geographic elements in different directions (Sun et al., 2020), so the TEDD between two periods was used to represent the expansion direction characteristics.

5. Conclusions

In this study, taking the urban land expansion process of Beijing from 1995 to 2015 as an example, we incorporated the influence of historical transition rules on urban land expansion into the simulation of the target period through linear smoothing and exponential smoothing. The ESI was proposed to measure the similarity of the urban expansion processes within the two periods, and smoothing weights were assigned to each period in accordance with the ESI to quantify the influence degree of each period. The SM-Logistic-CA model with a neighborhood decay effect was used to simulate the urban growth from 2010 to 2015, and the model using the transition rule extracted from 2010 to 2015 was treated as the benchmark to measure the effect of different smoothed rules. This study made full use of the historical transition rules of urban expansion to achieve a more realistic simulation. The main conclusions are as follows.

Whether the integration of historical transition rules can improve the simulation accuracy depends on two aspects. The first aspect is the similarity of the expansion processes between the historical period and the target period. Considering historical periods in which the expansion process was highly similar to that in the target period can help to achieve a more accurate simulation. Moreover, using transition rules extracted

from periods that differed significantly from the target period can make the simulation results worse. The second aspect is the temporal distance between the historical period and the target period. A historical period that is closer to the target time may have a greater impact on the simulation results, which could be more accurate or less accurate, depending on the level of similarity of the two periods. Furthermore, we found that the neighborhood size affects the dominance of the above two aspects. When the neighborhood size is small, the similarity between periods is more important for an accurate simulation. As the neighborhood size increases, the role of the temporal distance becomes stronger, and can even make up for the negative influence caused by the differences of the expansion processes. The findings of this study will contribute to an improved understanding of the urban land expansion process, and the research results will provide a reference for the temporal and spatial modeling of urban land evolution.

In addition, there are some problems that need to be studied in depth. Firstly, although the ESI proposed in this paper measures the similarity from multiple dimensions as much as possible, the process of urban expansion is complex, and indicators of other dimensions could be incorporated to further improve the ESI, after we obtain a deeper understanding of the urban expansion process. Secondly, we need to define a threshold for the ESI, within which the urban expansion processes of the historical period and the target research period are similar enough to each other so that scholars can believe that the transition rule of the historical period is beneficial to the simulation. This threshold may be different in different cities or regions, but a general threshold may also exist. Finally, although the two smoothing methods used in this study achieved encouraging results, we still need to try more methods to determine the smoothing weight of each period. Using intelligent and automated methods could greatly save the time spent in determining the optimal weight set. We will attempt to resolve these issues in a follow-up study.

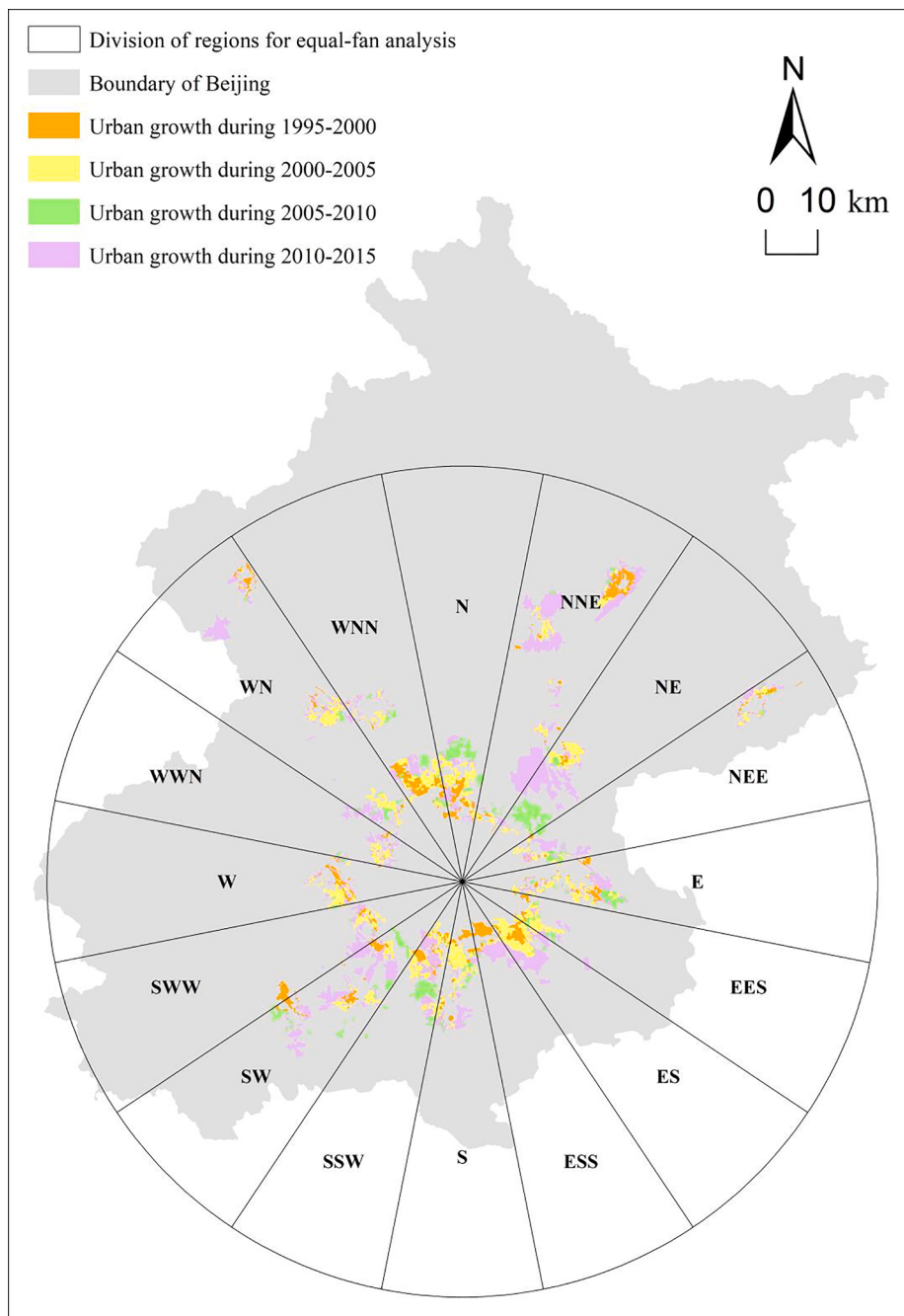
CRediT authorship contribution statement

Haijun Wang: Conceptualization, Funding acquisition, Methodology, Project administration, Resources, Supervision, Writing - original draft, Writing - review & editing. **Jiaqi Guo:** Conceptualization, Data curation, Formal analysis, Investigation, Methodology, Software, Validation, Visualization, Writing - original draft, Writing - review & editing. **Bin Zhang:** Investigation, Software, Writing - original draft. **Haoran Zeng:** Investigation, Writing - original draft.

Declaration of Competing Interest

The authors declare that they have no known competing financial interests or personal relationships that could have appeared to influence the work reported in this paper.

Appendix A. The region division of the equal-fan analysis.



Appendix B. The FoM values for all combinations of α and neighborhood size.

α	Neighborhood sizes							
	5 × 5	11 × 11	15 × 15	21 × 21	25 × 25	31 × 31	35 × 35	41 × 41
0.1	0.2064	0.2099	0.2129	0.2162	0.2176	0.2182	0.2178	0.2167
0.2	0.2082	0.2119	0.2150	0.2178	0.2188	0.2183	0.2176	0.2162
0.3	0.2086	0.2122	0.2144	0.2167	0.2172	0.2172	0.2166	0.2153
0.4	0.2090	0.2127	0.2153	0.2177	0.2186	0.2186	0.2178	0.2165
0.5	0.2075	0.2112	0.2138	0.2166	0.2176	0.2172	0.2163	0.2150
0.6	0.2071	0.2107	0.2135	0.2163	0.2176	0.2171	0.2163	0.2151
0.7	0.2066	0.2103	0.2131	0.2160	0.2177	0.2172	0.2167	0.2154
0.8	0.2059	0.2093	0.2121	0.2152	0.2168	0.2169	0.2165	0.2157
0.9	0.2049	0.2076	0.2103	0.2134	0.2149	0.2159	0.2159	0.2148

References

- Aburas, M. M., Ho, Y. M., Ramli, M. F., & Ash Aari, Z. H. (2016). The simulation and prediction of spatio-temporal urban growth trends using cellular automata models: a review. *International Journal of Applied Earth Observation and Geoinformation*, 52, 380–389. <https://doi.org/10.1016/j.jag.2016.07.007>.
- Agyemang, F. S. K., & Silva, E. (2019). Simulating the urban growth of a predominantly informal Ghanaian city-region with a cellular automata model: Implications for urban planning and policy. *Applied Geography*, 105, 15–24. <https://doi.org/10.1016/j.apgeog.2019.02.011>.
- Al-sharif, A. A. A., & Pradhan, B. (2013). Monitoring and predicting land use change in Tripoli Metropolitan City using an integrated Markov chain and cellular automata models in GIS. *Arabian Journal of Geosciences*, 7(10), 4291–4301. <https://doi.org/10.1007/s12517-013-1119-7>.
- Cadenas, E., Jaramillo, O. A. & Rivera, W. (2010). Analysis and forecasting of wind velocity in chetumal, quintana roo, using the single exponential smoothing method. *Renewable Energy*, 35(5), 925–930. <https://doi.org/10.1016/j.renene.2009.10.037>.
- Cao, Y., Zhang, X., Fu, Y., Lu, Z., & Shen, X. (2020). Urban spatial growth modeling using logistic regression and cellular automata: a case study of Hangzhou. *Ecological Indicators*, 113, 106200. <https://doi.org/10.1016/j.ecolind.2020.106200>.
- de Mesnard, L. (2013). Pollution models and inverse distance weighting: Some critical remarks. *Computational Geosciences*, 52(52), 459–469. <https://doi.org/10.1016/j.cageo.2012.11.002>.
- Divilgilpitaya, P., & Handayani, K.N. (2015). Measuring the urban expansion process of Yogyakarta city in Indonesia. *International Review for Spatial Planning and Sustainable Development*, 3(4), 18–32. <https://doi.org/10.14246/irspd.3.4.18>.
- Feng, Y., & Tong, X. (2018). Dynamic land use change simulation using cellular automata with spatially nonstationary transition rules. *GIScience and Remote Sensing*, 55(5), 678–698. <https://doi.org/10.1080/15481603.2018.1426262>.
- Feng, Y., Liu, Y., Tong, X., Liu, M., & Deng, S. (2011). Modeling dynamic urban growth using cellular automata and particle swarm optimization rules. *Landscape and Urban Planning*, 102(3), 188–196. <https://doi.org/10.1016/j.landurbplan.2011.04.004>.
- Feng, Y., Wang, R., Tong, X., & Shafizadeh-Moghadam, H. (2019). How much can temporally stationary factors explain cellular automata-based simulations of past and future urban growth? *Computers, Environment and Urban Systems*, 76, 150–162. <https://doi.org/10.1016/j.compenvurbsys.2019.04.010>.
- Fu, X., Wang, X., & Yang, Y. J. (2018). Deriving suitability factors for CA-Markov land use simulation model based on local historical data. *Journal of Environment Management*, 206, 10–19. <https://doi.org/10.1016/j.jenvman.2017.10.012>.
- Goodchild, M. F. (2004). The validity and usefulness of laws in geographic information science and geography. *Annals of the Association of American Geographers*, 94(2), 300–303. <https://doi.org/10.1111/j.1467-8306.2004.09402008.x>.
- Hargis, C. D., Bissonette, J. A., & David, J. L. (1998). The behavior of landscape metrics commonly used in the study of habitat fragmentation. *Landscape Ecology*, 13(3), 167–186. <https://doi.org/10.1023/A:1007965018633>.
- He, C., Okada, N., Zhang, Q., Shi, P., & Zhang, J. (2006). Modeling urban expansion scenarios by coupling cellular automata model and system dynamic model in Beijing, China. *Applied Geography*, 26(3–4), 323–345. <https://doi.org/10.1016/j.apgeog.2006.09.006>.
- Huang, B., Zhang, L., & Wu, B. (2009). Spatiotemporal analysis of rural-urban land conversion. *Int. J. Geogr. Inf. Sci.*, 23(3), 379–398. <https://doi.org/10.1080/13658810802119685>.
- Huang, D., Tan, X., Liu, T., Chu, E. & Kong, F. (2020). Effects of hierarchical city centers on the intensity and direction of urban land expansion: A case study of Beijing. *Land*, 9(9), 312. <https://doi.org/10.3390/land9090312>.
- Jiang, W., Wu, X., Gong, Y., Yu, W., & Zhong, X. (2020). Holt-Winters smoothing enhanced by fruit fly optimization algorithm to forecast monthly electricity consumption. *Energy*, 193, 807–814. <https://doi.org/10.1016/j.energy.2019.116779>.
- Juszczuk, P., Kozak, J., & Kania, K. (2020). Using similarity measures in prediction of changes in financial market stream data-Experimental approach. *Data & Knowledge Engineering*, 125, 101782. <https://doi.org/10.1016/j.dake.2019.101782>.
- Kocabas, V., & Dragicevic, S. (2006a). Assessing cellular automata model behaviour using a sensitivity analysis approach. *Computers, Environment and Urban Systems*, 30 (6), 921–933. <https://doi.org/10.1016/j.compenvurbsys.2006.01.001>.
- Kocabas, V., & Dragicevic, S. (2006b). Exploring the impacts of neighborhood size and type variations on gis-based cellular automata model: A sensitivity analysis approach. *IEEE*, 2445–2448. <https://doi.org/10.1109/IGARSS.2006.633>.
- Ku, C. (2016). Incorporating spatial regression model into cellular automata for simulating land use change. *Applied Geography*, 69, 1–9. <https://doi.org/10.1016/j.apgeog.2016.02.005>.
- Lastra-Díaz, J. J., Goikoetxea, J., Hadj Taieb, M. A., García-Serrano, A., Ben Aouicha, M., & Agirre, E. (2019). A reproducible survey on word embeddings and ontology-based methods for word similarity: Linear combinations outperform the state of the art. *Engineering Applications of Artificial Intelligence*, 85, 645–665. <https://doi.org/10.1016/j.engappai.2019.07.010>.
- Li, X., & Liu, X. (2006). An extended cellular automaton using case-based reasoning for simulating urban development in a large complex region. *International Journal of Geographical Information Science*, 20(10), 1109–1136. <https://doi.org/10.1080/13658810600816870>.
- Li, X., & Yeh, A. (2001). Calibration of cellular automata by using neural networks for the simulation of complex urban systems. *Environment and Planning A-Economy and Space*, 33(8), 1445–1462. <https://doi.org/10.1068/a33210>.
- Li, X., Zhou, Y., & Chen, W. (2020). An improved urban cellular automata model by using the trend-adjusted neighborhood. *Ecological Processes*, 9(1), 1–13. <https://doi.org/10.1186/s13717-020-00234-9>.
- Liao, J., Tang, L., Shao, G., Qiu, Q., Wang, C., Zheng, S., & Su, X. (2014). A neighbor decay cellular automata approach for simulating urban expansion based on particle swarm intelligence. *International Journal of Geographical Information Science*, 28(4), 720–738. <https://doi.org/10.1080/13658816.2013.869820>.
- Liao, J., Tang, L., Shao, G., Su, X., Chen, D., & Xu, T. (2016). Incorporation of extended neighborhood mechanisms and its impact on urban land-use cellular automata simulations. *Environmental Modelling & Software: With Environment Data News*, 75, 163–175. <https://doi.org/10.1016/j.envsoft.2015.10.014>.
- Liu, F., Zhang, Z., & Wang, X. (2016). Forms of urban expansion of Chinese municipalities and provincial capitals, 1970s–2013. *Remote Sensing*, 8(11), 930. <https://doi.org/10.3390/rs8110930>.
- Liu, X., Li, X., Chen, Y., Tan, Z., Li, S., & Ai, B. (2010). A new landscape index for quantifying urban expansion using multi-temporal remotely sensed data. *Landscape Ecology*, 25(5), 671–682. <https://doi.org/10.1007/s10980-010-9454-5>.
- Liu, X., Li, X., Liu, L., He, J., & Ai, B. (2008). A bottom-up approach to discover transition rules of cellular automata using ant intelligence. *International Journal of Geographical Information Science*, 22(11–12), 1247–1269. <https://doi.org/10.1080/13658810701757510>.
- Liu, Y., Fang, F., & Li, Y. (2014). Key issues of land use in China and implications for policy making. *Land Use Policy*, 40, 6–12. <https://doi.org/10.1016/j.landusepol.2013.03.013>.
- Ma, S., Liu, F., Ma, C., & Ouyang, X. (2020). Integrating logistic regression with ant colony optimization for smart urban growth modelling. *Frontiers of Earth Science*, 14 (1), 77–89. <https://doi.org/10.1007/s11707-018-0727-7>.
- McGarigal, K., & Marks, B. J. (1995). FRAGSTATS: Spatial pattern analysis program for quantifying landscape structure. U.S. Forest Service General Technical Report PNW-351. Pacific Northwest Research Station, Corvallis.
- Mirbagheri, B., & Alimohammadi, A. (2017). Improving urban cellular automata performance by integrating global and geographically weighted logistic regression models. *Transactions in GIS*, 21(6), 1280–1297. <https://doi.org/10.1111/tgis.12278>.
- Mustafa, A., Heppenstall, A., Omrani, H., Saadi, I., Cools, M., & Teller, J. (2018). Modelling built-up expansion and densification with multinomial logistic regression, cellular automata and genetic algorithm. *Computers, Environment and Urban Systems*, 67, 147–156. <https://doi.org/10.1016/j.compenvurbsys.2017.09.009>.
- Niesterowicz, J., & Stepinski, T. F. (2016). On using landscape metrics for landscape similarity search. *Ecological Indicators*, 64, 20–30. <https://doi.org/10.1016/j.compenvurbsys.2017.09.009>.
- Palmate, S. S., Pandey, A., & Mishra, S. K. (2017). Modelling spatiotemporal land dynamics for a trans-boundary river basin using integrated cellular automata and Markov chain approach. *Applied Geography*, 82, 11–23. <https://doi.org/10.1016/j.apgeog.2017.03.001>.
- Qian, Y., Xing, W., Guan, X., Yang, T., & Wu, H. (2020). Coupling cellular automata with area partitioning and spatiotemporal convolution for dynamic land use change simulation. *Science of the Total Environment*, 722, 137738. <https://doi.org/10.1016/j.scitotenv.2020.137738>.
- Roodposhti, M. S., Hewitt, R. J., & Bryan, B. A. (2020). Towards automatic calibration of neighbourhood influence in cellular automata land-use models. *Computers, Environment and Urban Systems*, 79, 101416. <https://doi.org/10.1016/j.compenvurbsys.2019.101416>.
- Sadeghi, A. (2015). Providing a measure for bullwhip effect in a two-product supply chain with exponential smoothing forecasts. *International Journal of Production Economics*, 169, 44–54. <https://doi.org/10.1016/j.ijpe.2015.07.012>.
- Santé, I., García, A. M., Miranda, D., & Creciente, R. (2010). Cellular automata models for the simulation of real-world urban processes: A review and analysis. *Landscape and Urban Planning*, 96(2), 108–122. <https://doi.org/10.1016/j.landurbplan.2010.03.001>.
- Shafizadeh-Moghadam, H., Asghari, A., Taleai, M., Helbich, M., & Tayyebi, A. (2017a). Sensitivity analysis and accuracy assessment of the land transformation model using cellular automata. *GIScience & Remote Sensing*, 54(5), 639–656. <https://doi.org/10.1080/15481603.2017.1309125>.
- Shafizadeh-Moghadam, H., Asghari, A., Tayyebi, A., & Taleai, M. (2017b). Coupling machine learning, tree-based and statistical models with cellular automata to simulate urban growth. *Computers, Environment and Urban Systems*, 64, 297–308. <https://doi.org/10.1016/j.compenvurbsys.2017.04.002>.
- Su, Y., Gao, W., Guan, D., & Su, W. (2018). Dynamic assessment and forecast of urban water ecological footprint based on exponential smoothing analysis. *Journal of Cleaner Production*, 195, 354–364. <https://doi.org/10.1016/j.jclepro.2018.05.184>.
- Sun, W., Shan, J., Wang, Z., Wang, L., Lu, D., Jin, Z., ... Yang, J. (2020). Geospatial analysis of urban expansion using remote sensing methods and data: A case study of Yangtze river delta, China. *Complexity*, 2020, 1–12. <https://doi.org/10.1155/2020/3239471>.
- Sun, X., Crittenden, J. C., Li, F., Lu, Z., & Dou, X. (2018). Urban expansion simulation and the spatio-temporal changes of ecosystem services, a case study in Atlanta metropolitan area, USA. *Science of the Total Environment*, 622–623, 974–987. <https://doi.org/10.1016/j.scitotenv.2017.12.062>.
- Tobler, W. R. (1970). A computer movie simulating urban growth in the detroit region. *Economic Geography*, 46, 234–240. <https://www.tandfonline.com/doi/abs/10.23707/143141?journalCode=recg20>.
- Tu, Y., Chen, B., Yu, L., Xin, Q., Gong, P., & Xu, B. (2021). How does urban expansion interact with cropland loss? A comparison of 14 Chinese cities from 1980 to 2015. *Landscape Ecology*, 36(1), 243–263. <https://doi.org/10.1007/s10980-020-01137-y>.

- Verburg, P. H., de Nijs, T. C. M., Ritsema Van Eck, J., Visser, H., & de Jong, K. (2004). A method to analyse neighbourhood characteristics of land use patterns. *Computers, Environment and Urban Systems*, 28(6), 667–690. <https://doi.org/10.1016/j.compenvurbsys.2003.07.001>.
- White, R., & Engelen, G. (2000). High-resolution integrated modelling of the spatial dynamics of urban and regional systems. *Computers, Environment and Urban Systems*, 24(5), 383–400. [https://doi.org/10.1016/S0198-9715\(00\)00012-0](https://doi.org/10.1016/S0198-9715(00)00012-0).
- Wu, F., & Yeh, A. G. (1997). Changing spatial distribution and determinants of land development in Chinese cities in the transition from a centrally planned economy to a socialist market economy: A case study of Guangzhou. *Urban Studies*, 34(11), 1851–1879. <https://doi.org/10.1080/0042098975286>.
- Wu, H., Zhou, L., Chi, X., Li, Y., & Sun, Y. (2012). Quantifying and analyzing neighborhood configuration characteristics to cellular automata for land use simulation considering data source error. *Earth Science Informatics*, 5(2), 77–86. <https://doi.org/10.1007/s12145-012-0097-8>.
- Wu, L., Liu, S., & Yang, Y. (2016). Grey double exponential smoothing model and its application on pig price forecasting in China. *Applied Soft Computing*, 39, 117–123. <https://doi.org/10.1016/j.asoc.2015.09.054>.
- Xia, C., & Zhang, B. (2021). Exploring the effects of partitioned transition rules upon urban growth simulation in a megacity region: A comparative study of cellular automata-based models in the Greater Wuhan Area. *GIScience & Remote Sensing*, Article 1933714. <https://doi.org/10.1080/15481603.2021.1933714>.
- Zhang, B., & Wang, H. (2021). A new type of dual-scale neighborhood based on vectorization for cellular automata models. *GIScience and Remote Sensing*, 58(3), 386–404. <https://doi.org/10.1080/15481603.2021.1883946>.
- Zhang, B., & Xia, C. (2021). The effects of sample size and sample prevalence on cellular automata simulation of urban growth. *International Journal of Geographical Information Science*, , Article 1931237. <https://doi.org/10.1080/13658816.2021.1931237>.
- Zhao, J., Zhu, C., & Zhao, S. (2014). Comparing the spatiotemporal dynamics of urbanization in moderately developed Chinese cities over the past three decades: Case of Nanjing and Xi'an. *Journal of Urban Planning and Development*, 141(4), 05014029. [https://doi.org/10.1061/\(ASCE\)UP.1943-5444.0000251](https://doi.org/10.1061/(ASCE)UP.1943-5444.0000251).
- Zheng, K., You, Z. H., Wang, L., Zhou, Y., Li, L. P., & Li, Z. W. (2020). DBMDA: A unified embedding for sequence-based miRNA similarity measure with applications to predict and validate miRNA-disease associations. *Molecular Therapy-Nucleic Acids*, 19, 602–611. <https://doi.org/10.1016/j.omtn.2019.12.010>.
- Zhou, L., Dang, X., Sun, Q., & Wang, S. (2020). Multi-scenario simulation of urban land change in Shanghai by random forest and CA-Markov model. *Sustainable Cities and Society*, 55, 102045. <https://doi.org/10.1016/j.scs.2020.102045>.
- Zhu, A., Lu, G., Liu, J., Qin, C., & Zhou, C. (2018). Spatial prediction based on Third Law of Geography. *Annals of GIS*, 24(4), 225–240. <https://doi.org/10.1080/19475683.2018.1534890>.
- Zhu, A., Lu, G., Zhou, C., & Qin, C. (2020). 地理相似性:地理学的第三定律? (Geographic similarity: The third law of geography?) *Journal of Earth Information Science*, 22 (04), 673–679. (in Chinese, with English abstract).
- Ziaeefaeayan, H., Moattar, M. H., & Forghani, Y. (2018). Land use change model based on bee colony optimization, Markov chain and a neighborhood decay cellular automata. *Natural Resource Modeling*, 31(2), e12151. <https://doi.org/10.1111/nrm.12151>.